Eur. Phys. J. Special Topics **223**, 1037–1044 (2014)

DOI: 10.1140/epjst/e2014-02154-6

THE EUROPEAN PHYSICAL JOURNAL SPECIAL TOPICS

Regular Article

Laser acceleration in novel media

T. Tajima

Department of Physics and Astronomy, University of California at Irvine, Irvine, CA 92697, USA

Received 13 March 2014 / Received in final form 24 March 2014
Published online XX May 2014

Abstract. With newly available compact laser technology [1] we are capable of producing 100 PW-class laser pulses with a single-cycle duration on the femtosecond timescale. With a fs intense laser we can produce a coherent X-ray pulse that is also compressed, well into the hard X-ray regime (∼10 keV) and with a power up to as much as 10 Exawatts. We suggest utilizing these coherent X-rays to drive the acceleration of particles. Such X-rays are focusable far beyond the diffraction limit of the original laser wavelength and when injected into a crystal it forms a metallic-density electron plasma ideally suited for laser wakefield acceleration. If the X-ray field is limited by the Schwinger field at the focal size of ∼100 nm, the achievable energy is 1 PeV over 50 m. (If the X-rays are focused further, much higher energies beyond this are possible). These processes are not limited to only electron acceleration, and if ions are pre-accelerated to beyond GeV they are capable of being further accelerated using a LWFA scheme [2] to similar energies as electrons over the same distance-scales. Such high energy proton (and ion) beams can induce copious neutrons, which can also give rise to intense compact muon beams and neutrino beams that may be portable. High-energy gamma rays can also be efficiently emitted with a brilliance many orders of magnitude above the brightest X-ray sources by this accelerating process, from both the betatron radiation as well as the dominant radiative-damping dynamics. With the exceptional conditions enabled by this technology we envision a whole scope of new physical phenomena, including: the possibility of laser self-focus in the vacuum, neutron manipulation by the beat of such lasers, zeptosecond spectroscopy of nuclei, etc. Further, we now introduce along with the idea of vacuum as a nonlinear medium, the Schwinger Fiber Accelerator. This is a self-organized vacuum fiber acceleration concept, in which the repeated process of self-focusing and defocusing for the X-ray pulse in vacuum forms a modulated fiber that guides the intense X-rays.

1 Introduction

Contemporary accelerator technology is based on radio frequency (rf) electromagnetic waves in vacuum tubes [3, 4]. This technology has already served well for several decades in high energy physics as well as in applications such as medical therapy. However, it is increasingly apparent that the so-called Livingston chart in which the

accelerator energies exponentially increase in time (akin to Moore's law for semiconductor chip capabilities) [3,4] tends to show slower growth (and even a saturation tendency). This is because the accelerating gradient in rf accelerators has a limit beyond which the metallic surface of the rf tube begins to spark and the metal breaks down to create a plasma inside the tube. Such an accelerating gradient is typically limited to about 100 MeV/m. On the other hand, a laser wakefield accelerator (LWFA) [2] and its derivatives, such as plasma wakefield accelerators, use an ionized gas plasma, as the medium of acceleration and therefore do not suffer from the typical material breakdown constraint. This freedom allows for accelerating gradients far greater than conventional rf accelerators with typical accelerating gradients for LWFA of the order of 100 GeV/m (and other plasma wakefield accelerators range from 1–10 GeV/m). These gains are approximately one to four orders of magnitude greater than the existing rf accelerators.

The development of Chirped Pulse Amplification (CPA) [5] technique for laser technology has allowed for the creation of pulses with increasing peak powers within decreasing temporal durations. The advent and availability of such energetic laser pulses have allowed for the scientific verification of LWFA many times over as reviewed by [6]. The typical acceleration gradient observed in experiments confirms the predicted value near 100 GeV/m with typical energy gains of 1 GeV over a few cm. The scaling of the theoretical energy gain with the plasma density is also clearly seen. It is also understood that in order to increase the energy gain from GeV to 100 GeV, we have to increase the laser energy from the Joule-level to a 100–1000 J class laser system. A recent CERN Courier issue (November, 2013) featured not just one but three articles highlighting the latest initiatives on wakefield acceleration including both scientific and laser technological progress. We are in an exciting era to see the fruition of this concept to the real world accelerator, both in high energy acceleration and societal applications.

In this paper, considering the new developments in the laser technology for efficient pulse compression into the regime of fs (single oscillation in the pulse) along with larger available powers (such as PW-10 PW) [1], we introduce the concept of a much higher energy acceleration using LWFA with a compressed high intensity X-ray pulse. The typical compression by this method is capable of turning an optical laser (10 PW with 200 J, 20 fs laser) into a coherent X-ray source containing up to 10 keV energy photons within a single oscillation period of less than an attosecond. For a 20 EW pulse this represents about 20 J of X-rays. With such ultrahigh power X-rays, one can introduce LWFA within the regime of solid targets rather than gas. In the following several versions of this idea are described.

2 Crystal LWFA

Converting from the near-infrared frequencies of an ultrashort laser pulse [1] to the higher frequency of hard Xray photons enables one to drive wakefields in higher density matter than the typical gas plasmas. The high intensity LWFA energy gain is given by

$$\varepsilon_e = 2a_0^2 mc^2 (n_c/n_e), \tag{1}$$

where a_0 is the normalized vector potential of the laser electric field, n_c is the critical density of the plasma at the laser frequency, and n_e is the electron density [7]. In LWFA the higher the density of the medium, *i.e.* plasma, the greater the acceleration gradient becomes. However, with an increase of the density for the fixed laser frequency, the energy gain by LWFA decreases [2]. In order to avoid this energy loss with increasing density, it helps to raise the critical density – specifically through its

dependence on the laser wavelength: for 1 eV optical photons, n_c is about 10^{21}/cc, while the critical density for photons of 10 keV X-rays (we use the symbol n_{Xc}) is of the order 10^{29}/cc. (We will discuss our suggested method how to realize intense X-rays in the next paragraph). Therefore, by using X-rays to drive the LWFA introduces a tremendous gain in the attainable energy according to (1) because it is possible to use a solid-density electron plasma with a typical value of 10^{23}/cc. The accelerating length L_{acc} is

$$L_{acc} \sim a_X(c/\omega_p)(\omega_X/\omega_p)^2, \tag{2}$$

where ω_X is the X-ray frequency, and ω_p is the plasma frequency of the solid as seen by the X-ray photons (The photon frequency determines which of the deeply bound electrons may be regarded as the 'plasma electrons' for the X-ray photons). Here a_X is the normalized vector potential of the X-rays, and is related to the a_0 of the optical laser. The crystal LWFA energy gain is thus

$$\varepsilon_X = 2a_X^2 mc^2(n_{Xc}/n_e), \tag{3}$$

if we do not focus the X-rays below the radius of the optical laser focal size, $a_X \sim a_0$ (ω_0/ω_X), where ω_0 is the optical photon frequency. Here n_{Xc} is the critical density for the X-rays.

As the diffraction limit of the X-ray focal size can, in principle, be on the order of the X-ray wavelength, the maximum possible value a_X is not as small as the value above, but, with the reduction of the focus by the factor of (ω_0/ω_X), it remains as $a_X \sim a_0$ in the extreme optimal case for the X-ray focusing. If we take as an example the focal size of the X-rays between the two extremes (1μ and 0.1 nm), and assume an achievable focal size of 100 nm, the intensity at focus is approximately at the Schwinger intensity, if the X-rays are generated by the λ^3 mechanism of Naumova et al. [8]. Naumova's mechanism requires the optical laser be compressed temporally and spatially to the limit of the wavelength and upon interaction with a solid target surface results in further compression and up-conversion as the pulse reflects off as a single-cycle, higher frequency coherent photon pulse with the pulse duration given as

$$\tau_X \sim 600/a_0, \tag{4}$$

where τ_X is given in the unit of as [8]. In other words, the X-ray pulse power goes up by this compression by the factor of approximately a_0^2 over that of the original optical laser power. Assuming even a conversion efficiency of 0.1, an original nearly 200 J optical laser at 2 fs now becomes a coherent X-ray laser at 10 EW. In this example, the energy gain by the LWFA mechanism using X-rays at 10 keV in a solid crystal electronic density of 10^{23}/cc is found from Eq. (3) to be: $\varepsilon_X \sim 1$ PeV with Eq. (2) giving an acceleration length of $L_{acc} \sim 50$ m.

In the above estimate the electron energy loss by various mechanisms, including Bremsstrahlung and betatron radiation, has been neglected, while recognizing that, in reality, these radiations become very important [9,10]. In addition, a host of other quantum mechanical processes, such as pair creation, become important factors affecting the potential energy gain. However, it is known that the betatron radiation can contribute to the cooling of the transverse emittance and helps to potentially enhance the luminosity [10]. An accurate assessment of the potential mechanisms for the saturation of the electron acceleration process is needed in the near future to fully understand this method's potential.

In order to overcome the potentially large electron (and positron) energy loss in the crystal, we suggest the adoption of a nanohole (a nanometer-sized, or an even narrower few Angstrom-sized, tube) in the crystal which acts as a conduit to guide the transmission of the electrons and positrons, while the X-rays, as in the above

example, propagate over a wider radial cross section of typically 100 nm. However, if we can manage to focus X-rays onto even smaller radius or due to the relativistic self-focus in the crystal (the critical power at ∼20 PW at the 10 keV photon energy, which is much less than 10 EW), the corresponding value of a_X becomes greater than the value we used in the above estimate of $a_X \sim 30$. Thus the value of the gained energy and accelerating distance in Eqs. (3) and (2) become much greater than the values we estimated above. Again here applies the caution that the radiation energy loss processes etc. may become substantially greater and may become a central issue. More research is needed here. Also we refer more discussion on this to Sect. 6. If these processes may be restricted by the technique of the hollow crystal with nanohole, it may not be impossible to look at truly cosmic ray acceleration parameters of energy gains.

It may be argued that at the Schwinger intensity (or even below that value) of the X-rays (or optical) lasers the pair creation process becomes so dominant that no field intensity above this value may be realizable. If this is the case, the enhanced energy gain beyond the value we estimated in the paragraph two before this may not be surpassed. However, we suggest here that this seeming ultimate limit of the laser field intensity at the Schwinger value may be lifted by noting the following. Because the Poincare invariants E^2–B^2 and $\boldsymbol{E} \bullet \boldsymbol{B}$ remain Lorentz invariant if there is only one EM wave in a plane 1D geometry, such a wave cannot break down the vacuum. Thus we may be able to conduct the transmission of above Schwinger wave without much breakdown of vacuum if we satisfy the above condition (or approximately that condition). The kind of estimate we mentioned above in that paragraph for 10 nm focus, for example, may allow near 1D geometry so that the case in study may be close to such situation. If so, the field above that is attainable, at least theoretically. Here we note that the self-focusing condition in vacuum (for example, see [12]) may be fulfilled if the power of the laser P exceeds the critical power defined by

$$P_{cr} = (45/14)cE_S^2\lambda^2\alpha^{-1}, \tag{5}$$

where $E_S = 2\pi m^2c^3/eh$ is the Schwinger field and α is the fine structure constant. This value is as high as a few times 10^{24} W for optical lasers. However, for 10 keV X-rays, it is merely 25PW because of the square dependence of the wavelength of the driver in Eq. (5). Thus it may be possible to realize the self-focus of our X-rays laser pulse. This could further enhance our parameters estimated above.

3 Ultracompact high energy proton and ion acceleration in LWFA in a crystal

The arrangement we described for the crystal X-ray LWFA acceleration of electrons (and positrons) may be applied to proton acceleration. Here we illustrate the specific example of the method introduced by Zheng et al. [13,14]. This is the two-step LWFA method assisted by the radiation pressure driven injector. In this scheme the first thin solid foil plays the role of ion injector that is by the radiation pressure acceleration process [15]. This process may be driven either by the compressed optical pulse or the subsequently compressed X-rays pulse. This is because in the case of the usage of a 10 PW optical laser at 20 fs allows us to access the value of a_0 in excess of the mass ratio of proton-to-electron M/m, so that the optically compressed pulse at 2 fs is sufficient to accelerate protons (and ions) immediately relativistic regime that makes proton acceleration similar to electron acceleration at the entry of the relativistic optics of 10^{18} W/cm^2. Once the thin foil allows to inject protons (or ions) with relativistic energy into following LWFA that is driven by the above Sect. 2

process in the crystal, ions are accelerated just similarly to that described in Sect. 2. The formulas Eqs. (3) and (2) for the energy gain and the acceleration length apply equally well for ion acceleration (the energy gain of ions is the charge of ions Q times that of electrons).

The radiativeness of protons and ions is far smaller than electrons (mostly negligible in our parameters of relevance). Thus the kind of process and its corresponding formulas Eqs. (3) and (2) we discussed without radiative effects should be more reliable that that for the electron case. This opens up an entirely new prospect to consider proton or ion linear accelerators and its based collider. For such a new process we need to now consider the luminosity issue without the allowance of ring accumulation that is typical of hadron colliders. On the other hand, this allows a compact linear accelerator for protons and ions for lower energy applications. These include the following applications discussed in the Sects. 4 and 5.

4 Ulracompact neutron source

It is not so difficult to achieve relativistic protons or ions without the second step of the above two step ion acceleration approach, as the laser intensity is so high at the compressed optical laser before we resort to the X-ray compression step. Using the radiation pressure acceleration scheme of [12], we can access to relativistic protons (and ions) without resorting to the crystal X-ray acceleration step. This allows us to produce relativistic neutrons primarily propagating in the forward direction with a narrow spreading angle. The distance over which we can produce such neutrons can be less than mm with the kind of laser intensity mentioned.

5 Ultracompact muon and neutrino sources and muon linear collider; portable earth exploration muon and neutrino sources

Access to highly relativistic neutrons in an instantaneous fashion over extremely short distances allows for their application in making relativistic muon or neutrino beams with the method as described in [16]. The relativistic muon beams generated in this manner may then be injected into the crystal LWFA accelerator brought to extreme high energies in a linear fashion. The energy gain and the acceleration length for muons are similar to Eqs. (2) and (3). However, one important difference is that muon are nearly 200 times heavier than electrons so that the radiative energy loss for muons is many orders of magnitude less than that of electrons. Because muons are fundamental particles, the resultant muon linear collider may act as fantastically (or more so) as an electron-positron collider of the same energy. The described muon linear collider does not suffer from the radiative activation of the surrounding circular walls of the muon ring that prepare for the collision events, because the main radiative activation stems from muon decay in the direction tangent to the muon orbit. For the linear muon accelerator the activation radiation due to decay remains in the muon propagation direction and thus can be limited only to the small forward steradian.

Both the muon beams and neutrino beams emanating from this scheme can be produced in a laser that can fit (in principle) to a portable size and the accelerating distance is modest when compared to the size of a laser system. This implies that a portable muon source and neutrino source can be produced which allows for the following unprecedented capabilities. The muon beam may be very useful in diagnosing the constituent isotopes of dense materials (for example, exposed radioactive spent fuel, such as at the Fukushima plant) [17]. The interaction length of high energy muon beams is intermediate and much longer than that of electrons while not being on such

a large distance scale as to be impractical. This allows the apparatus to be sufficiently far removed for situations requiring remote sensing such as with imminent radiative threats, again like Fukushima.

Meanwhile, a neutrino beam provides entirely new possibilities because the neutrino interaction length is macroscopic on the scale of several thousand km even with dense matter. This makes neutrino beams particularly well-suited as probes of the earth's interior and a portable neutrino source would allow for a CT scan of both the earth's crust and its deeper core. The former would bring unprecedented global information on the geology of minerals, water, and other deposits (such as oil and gas), as well as the earth geologic structure (such as seismological information). The deep interior structure obtainable from neutrino beams will assist our understanding of planetary genesis and evolution as well as precise knowledge of the interior materials.

6 Ultraintense and ultrahigh energy gamma beam sources

Both the compressed, intense optical laser pulse and the highly accelerated electrons in the crystal by the derived X-rays are capable of generating bright and sometimes even coherent high energy photons via a variety of processes. First, the radiative damping effects are expected to become important beyond the laser intensity of $10^{23}\,\mathrm{W/cm^2}$ [18–20]. Beyond this threshold there is the expectation of highly efficient gamma ray generation directly from the radiative damping mechanisms for the electrons. In addition to this we already know that there is a very efficacious radiative process via the betatron radiation during the LWFA [9,10,21,22]. It is shown in [22] that the LWFA driven betatron radiation can exceed the third-generation large synchrotron radiation facilities in their instantaneous brilliance by a large margin. Thus it is quite promising to pursue ultracompact, ultrabright, ultrafast gamma beam sources by intense laser-driven radiative processes.

7 Neutron manipulation by intense lasers

The ultraintense optical laser like the one our scheme allows permits us to explore the interaction with neutrons. Neutrons are charge neutral. This is may be regarded as not possible to make interection with lasers. However, neutrons do have tiny but finite magnetic moment. Latching on this magnetic moment of neutrons, it becomes possible to kick neutron by lasers: the intensity of our compressed optical laser mentioned beyond $10^{25}\,\mathrm{W/cm^2}$ is enough that begins influencing the dynamics of even chargeless neutrons. Neutron's tiny but finite magnetic moment can interact with magnetic field gradient with sufficiently strong EM intensity at or beyond $10^{25}\,\mathrm{W/cm^2}$ [23]. This way we now provide a concrete way to manipulate cold neutrons (typical energy $3\times10^{-3}\,\mathrm{eV}$ with a beat wave of two intense lasers at intensity of $10^{25}\,\mathrm{W/cm^2}$ realizable by the optical laser compressed in to 2 fs by the method of [1]) by intense lasers for the first time.

8 Schwinger fiber accelerator

The intense X-ray laser pulse enables a new way to accelerate particles such as electrons and positrons while avoiding the materials limitations that surround the accelerator tubes in conventional rf accelerators and employs plasmas as the accelerating medium in a wakefield accelerator scheme. At a certain power of the X-ray laser, the beam begins to self-focus. If this happens, the rays of the X-rays begin to converge

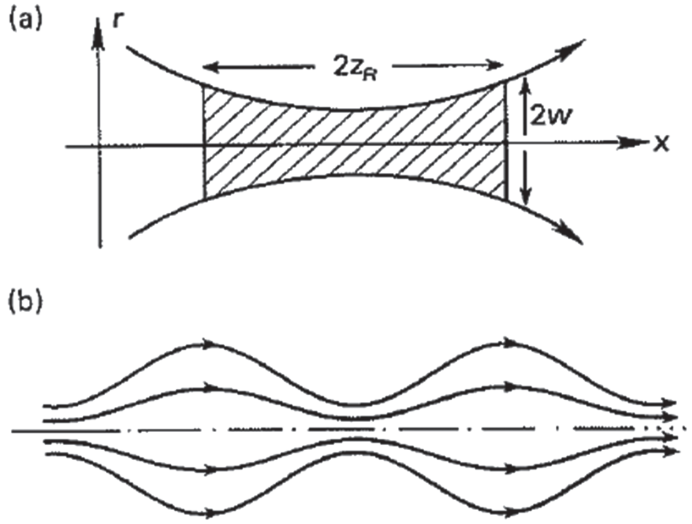

Fig. 1. The linear process of the Rayleigh diffraction over the Rayleigh length of z_R with waist w (a); the nonlinear processes of the self-focus, diffraction, and defocus and their repetitions (b). After [24].

until it reaches the size to now diffract. Such a size is the Rayleigh length z_R given by $z_R = \pi w_0^2/\lambda_i$, where w_0 is the waist size and λ_l is the laser wavelength. The Rayleigh length is tied to the focal length. Thus after the Rayleigh length, the X-ray laser begins to diffract and defocuses. After such defocus, it undergoes the previous self-focus again and may repeats the above self-focus and diffract and defocus processes again and again. This would constitute a laser fiber accelerator configuration akin to [24]. See Fig. 1.

Once this self-focus, diffraction, and defocus process begins, the local phase velocity of the X-ray laser ω/k_z is generally greater than c. Here the dispersion relation of the laser is determined as

$$\omega = c\sqrt{(k_z^2 + < k_{perp}^2 >)}, \tag{6}$$

where $< k_{perp}^2 >$ is the average of the square of the perpendicular wavenumber k_{perp} that changes as the laser propagation undergoes the above process of self-focus and diffraction. In order to match the phase velocity of the accelerating structure with the particle velocity (c), we need to introduce a slow wave structure by this self-focusing dynamics (see Fig. 1b) with the slow wave corrugation wavenumber k_s satisfying the condition [25]:

$$\omega/(k_z + k_s) = c, \quad k_s = 2\pi/s. \tag{7}$$

The length s is determined by the repeated succession of self-focusing and diffraction, which produces the periodicity of this repetition. The exact condition to choose the entrant X-ray laser focusing for satisfying Eq. (7) may need to be determined by numerical QED simulation, sophisticated theory, or eventually experiments in the future study to ascertain the process.

9 Conclusions

Intense single oscillation optical laser compression [1] allows for a regime of laser acceleration driven by an induced intense X-ray laser. This X-ray pulse is so intense that

we have introduced at least two ways to make use of this for the purpose of acceleration processes. One is to inject these intense X-rays into a crystal to cause wakefields (LWFA). The LWFA is excited in the sea of crystal electrons, whose parameters far exceed those realizable in gaseous plasma wakefield acceleration. We introduce its applications not only to electron acceleration, but also ions and subsequently a variety of particles. The second application for this intense X-ray laser was its injection into vacuum, where the field strength may be sufficient to now access the nonlinear property of empty space and allow us to use vacuum as a medium. X-ray lasers may begin to (figuratively speaking) "swim in the sea" of vacuum in a way akin to other media. If so, we foresee the possibility of a plasma fiber accelerator now in vacuum in the image of Schwinger.

The author benefited from the valuable and inspiring discussion with Gerard Mourou on [1] as well as the general aspects of the applications and with A. Chao on use of X-rays, while he also appreciates the careful reading of the manuscript by Jonathan Wheeler. The work was supported by the Norman Rostoker Fund at UCI.

References

1. G. Mourou, S. Mirnov, E. Khazanov, A. Sergeev, Single Cycle Thin Film Compressor Opening the Door to Zeptosecond-Exawatt Physics EPJ (submitted) (2014)
2. T. Tajima, J.M. Dawson, Phys. Rev. Lett. **43**, 267 (1979)
3. M. Livingston, J. Blewett, *Particle Accelerators* (McGraw-Hill, New York, 1962)
4. A. Chao, M. Tigner, *Handbook of Accelerator Science and Technology* (World Scientific, Singapore, 1999)
5. D. Strickland, G. Mourou, Opt. Comm. **56**, 219 (1985)
6. E. Esarey, et al., Rev. Mod. Phys. **81**, 1229 (2009)
7. T. Tajima, Proc. Jpn. Acad. Ser. B **86**, 147 (2010)
8. N. Naumova, et al., PRL **93**, 195003 (2004)
9. K. Nakajima, et al., PR STAB **14**, 091301 (2011)
10. A. Deng, et al., PR STAB **15**, 081303 (2012)
11. B. Newberger, T. Tajima, F.R. Huson, W. Mackay, B.C. Covington, J.R. Payne, Z.G. Zou, N.K. Mahale, S. Ohnuma, *Application of Novel Material in Crystal Accelerator Concepts*, Proc. IEEE Part. Acc. (IEEE, Chicago, 1989), p. 630
12. G. Mourou, et al., Rev. Mod. Phys. **78**, 309 (2006)
13. F.L. Zheng, H.Y. Wang, X.Q. Yan, J.E. Chen, Y.R. Lu, Z.Y. Guo, T. Tajima, X.T. He, Phys. Plasmas **19**, 023111 (2012)
14. F.L. Zheng, et al., Phys. Plasmas **20**, 013107 (2013)
15. T. Esirkepov, M. Borghesi, S.V. Bulanov, G. Mourou, T. Tajima, Phys. Rev. Lett. **92**, 175003 (2004)
16. F. Terranova, S. Bulanov, T. Esirkepov, P. Migliozzi, F. Pegoraro, T. Tajima, Nucl. Phys. B-Proc. Suppl. **143**, 572 (2005)
17. "Nuclear Physics and Gamma-ray Sources for Nuclear Security and Nonproliferation" (Tokai, Japan, 2014) `www.jaea.go.jp/english/npnsnp/NPNSNP%20Program`
18. A. Zhidkov, et al., Phys. Rev. Lett. **88**, 185002 (2002)
19. J. Koga, S. Bulanov, T. Esirkepov, in *Ultrafast Optics V* (2007)
20. A. Di Piazza, C. Mueller, K. Hatsagortsyan, C. Keitel, Rev. Mod. Phys. **84**, 1177 (2012)
21. S. Corde, et al., Rev. Mod. Phys. **85**, 1 (2013)
22. Y. Ma, L.M. Chen, M. Chen, W.C. Yan, D.Z. Li, K. Huang, Z.M. Sheng, K. Nakajima, T. Tajima, J. Zhang, Nature Photon. (submitted) (2014)
23. T. Tajima, K. Soyama, J. Koga, H. Takuma, J. Phys. Soc. Jpn. **69**, 3840 (2000)
24. T. Tajima, Laser Part. Beams **3**, 351 (1985)
25. T. Tajima, M. Cavenago, Phys. Rev. Lett. **59**, 1440 (1987)